Quasi-Ballistic Transport in Nano-Scale Devices: Boundary Layer, Potential Fluctuation, and Coulomb Interaction

Nobuyuki Sano
Institute of Applied Physics
University of Tsukuba
Tsukuba, Japan
sano@esys.tsukuba.ac.jp

***Abstract*—The singular nature of the Boltzmann transport equation leads to the boundary layer around the virtual source in nano-scale device structures. We show that the boundary layer is a key concept to understand the physical mechanism behind quasi-ballistic transport in nano-scale devices. The self-consistent 3D Monte Carlo device simulator is constructed by including accurately the full Coulomb interaction. It is shown that that the boundary condition for the electron distribution function plays an essential role to obtain the correct transport characteristics and that the Coulomb interaction is indeed a key ingredient for reliable predictions of device properties.**

I. INTRODUCTION

It is now well recognized that simply scaled Si MOSFETs do not exhibit any performance improvement in deca-nanometer regimes and, as a result, the introduction of technology boosters such as strain or alternate materials in the channel region is inevitable to gain the merit of "scaling" [1]. Nevertheless, the origin of the performance degradation is still unclear and usually attributed to additional scattering due to impurities and/or the surface-roughness, or parasitic resistance. Recently, it was pointed out that the trend of device performance degradation is remarkably similar to that due to the Coulomb interaction [2]. Here, we would like to stress that there are two questions to be addressed: One is why scattering is inevitable even in single nano-scale channels. The other is how quantitatively the scattering (interaction) affects device performance in nano-scale devices.

In the present paper, we discuss both problems by the two different means; by purely theoretical analyses under the relaxation time approximation and by numerical Monte Carlo (MC) simulations. We show that scattering is continued to be inevitable even in single nano-scale devices due to the boundary layer formed near the virtual source in the channel and that the accurate incorporation of the Coulomb interaction into 3D MC simulations is essential for reliable predictions of device characteristics.

This research is funded in part by Grants-in-Aid for Scientific Research (B) (No.2160160) from the Ministry of Education, Culture, Sports, Science, and Technology in Japan.

II. BOUNDARY LAYER STRUCTURE

A. Singularity of the Boltzmann Trasport Equation

The concept of the boundary layer (BL) arises from the fact that the Boltzmann transport equation (BTE) is singular with respect with the relaxation time and velocity [3].

Under the relaxation time approximation, the formal solution of the BTE under steady state is given by

$$f(x) = e^{-\int_{x_0}^{x} \frac{dx'}{v(x')\tau(x')}} f(x_0) + e^{-\int_{x_0}^{x} \frac{dx'}{v(x')\tau(x')}} \int_{x_0}^{x} dx'' \left\{ \frac{f_{eq}(x'')}{v(x'')\tau(x'')} e^{\int_{x_0}^{x} \frac{dx'''}{v(x''')\tau(x''')}} \right\}, \quad (1)$$

where $f(x)$ is the velocity distribution at position x, $v(x)$ is the electron velocity, and $\tau(x)$ is the position-dependent relaxation time. $f_{eq}(x)$ is the local thermal-equilibrium distribution and given by either the Maxwell-Boltzmann or the Fermi-Dirac distribution. The first term represents the ballistic component damped with the relaxation time τ and the second term represents the diffusive component due to scattering and thermalization. Since the distribution is ought to relax to local thermal-equilibrium, the relaxation time approximation employed here represents both elastic and inelastic scattering. This is a crucial difference from [4] where only elastic scattering is involved in their analyses.

It should be noticed that the relaxation time τ does not appear singly in (1), but rather, it is always paired with velocity v. This implies that the ballistic limit corresponding to taking the limit of $\tau \to \infty$ cannot be naively taken. In fact, the velocity could be as small as zero near the bottom of the conduction band and (1) becomes singular as $v\tau \to 0$. This leads to a peculiar behavior in the velocity distribution $f(x)$ near the singularity, as explained in the followings.

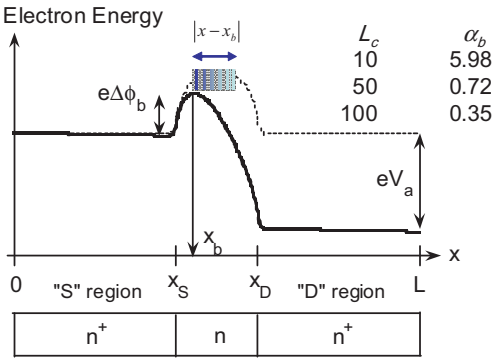

Fig.1. Device (n^+-n-n^+) structure used for the analyses of the BTE. The shaded region around the top of the potential barrier represents the BL.

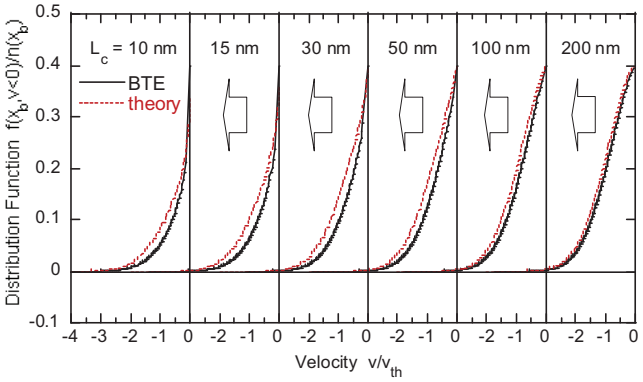

Fig.2. Velocity distributions from the analytical and numerical solutions of the BTE under the relaxation time approximation.

B. *Intrinsic Ballistic Parameter*

The mathematical structure of the BTE becomes clearer if the BTE is normalized.

To be more specific, let us consider a simple n^+-n-n^+ structure, as depicted in Fig. 1 where the potential profile along the channel direction is sketched. The normalized BTE naturally leads to a parameter α_b which is intrinsic to the BTE and expressed as

$$\alpha_b = \frac{e\tau^2 V''(x_b)}{2m}, \tag{2}$$

where e is the elementary charge, m is the effective mass, $V''(x_b)$ is the second derivative of the electrostatic potential at the top of the potential barrier x_b in the n (hereafter, denoted as channel) region (Fig. 1).

A rough estimation of α_b makes its physical implication clear; $\alpha_b \approx v_d \tau / L_c$, where L_c is the channel length and v_d is the drift velocity along the channel direction. Therefore, α_b represents the ballisticity of electron transport. Typical values of α_b extracted from the potential profiles found from the Drift-Diffusion simulations are listed in the inset to Fig. 1. The most important feature of (2) is that α_b is dependent of the curvature of $V(x)$. This implies that electron transport is intimately nonlocal, i.e., dependent of the functional $V(x)$, and its nonlocality becomes significant as L_c shrinks.

C. *Characteristic Region: Boundary Layer*

The intrinsic parameter α_b introduces the characteristic region $|x-x_b|$ in the channel, within which the electrons suffer higher probabilities to be scattered. This region denoted as the boundary layer (BL) depends on α_b as

$$|x-x_b| = v_{th}\tau_c \sqrt{\frac{\bar{\delta}}{\alpha_b}}, \tag{3}$$

where $\bar{\delta}$ is the kinetic energy measured from the top of the potential barrier at x_b (normalized by the thermal energy kT) and v_{th} is the thermal velocity. The electrons in the BL region suffer scattering and thermalization. The scattering processes in the BL are in fact much involved. The back-scattering dominates around the boundary of the BL region, and the thermalization dominates inside the BL region. The former is strongly dependent of the boundary condition of $f(x)$ at the channel/drain or channel/source junction and contributes to the current, whereas the latter gives rise to nearly no current [3]. Furthermore, it should be pointed out that the size of the BL region depends on the kinetic energy. The larger the kinetic energy, the longer the BL so that the electrons injected from the source with large kinetic energy have higher chances to be back-scattered in the BL region.

It is easy to show that the size of the kT-layer proposed in [5] is expressed by

$$L_{kT} \approx \sqrt{\frac{2kT}{eV''(x_b)}} \approx \frac{v_{th}\tau_c}{\sqrt{\alpha_b}}. \tag{4}$$

Comparing (4) with (3), we find that the kT-layer corresponds to the BL when electron's kinetic energy is given by the thermal energy kT. In other words, if the electrons in the source region are highly degenerate, which is the case in most cases, the kinetic energy of injection electrons at the virtual source is much larger than kT, and the energy dependence of the layer should be taken into account. In addition, the physical mechanism implied by the kT-layer theory is very different from the present BL model, as described in [3].

Analytical expression of the velocity distribution for the BTE is obtained under the relaxation time approximation and the velocity distributions are plotted with the numerical solutions in Fig. 2 for various channel lengths L_c. The velocity distributions for the negative velocity regions which represent the electrons scattered in the channel region are shown. The negative velocity components do not diminish as L_c shrinks even to 10 nm and this finding results from the singularity of the BTE. We must conclude that there is no ballistic limit due to the singularity of the BTE and a naïve picture of ballistic transport is rather misleading.

III. 3D Monte Carlo Simulation and the Coulomb Interaction

The analyses in the previous section are based on the relaxation time approximation and electron transport in nano-scale devices is actually much more complicated. In order to

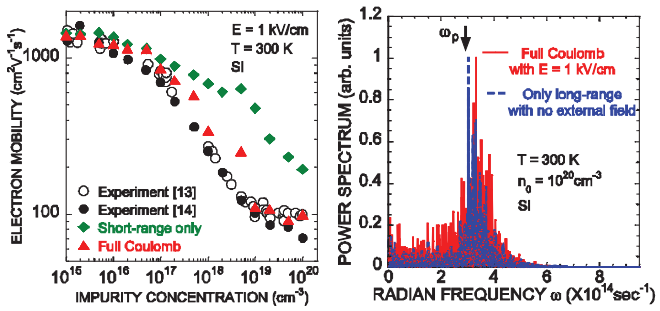

(a) (b)

Fig.3. (a) Electron mobility under various impurity concentrations and (b) Power spectrum calculated from the potential fluctuations.

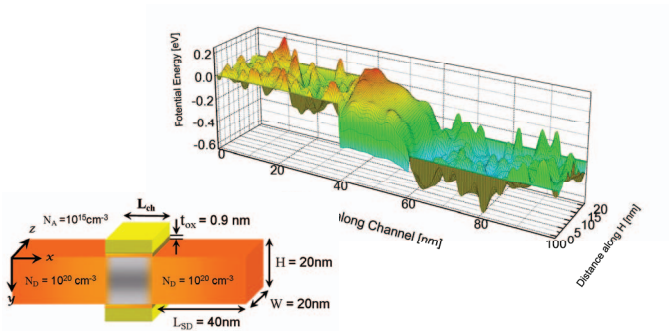

(a) (b)

Fig.4. (a) DG-MOSFET structure employed for the simulations and (b) Snapshot of potential configuration obtained from the MC simulations.

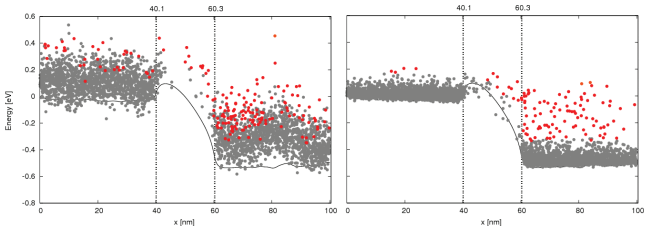

(a) (b)

Fig.5. Spatial distribution of electrons as a function of kinetic energy obtained from (a) self-consistent MC and (b) MC under fixed potential.

investigate the device performance quantitatively, we need to rely on time-consuming numerical simulations.

As pointed out in the previous section, the boundary condition of the velocity distribution $f(x,v)$ at both edges of the channel is most important to determine $f(x,v)$ in the channel region. In other words, it is essential to simulate electron transport not only in the channel region but also in the source and drain regions to get the correct velocity distribution $f(x,v)$. The most important interaction in highly doped source and drain is the electron-electron and electron-impurity scattering through the Coulomb interaction. However, the incorporation of the Coulomb interaction in particle-based simulations is a long-standing problem. It been tackled with various techniques such as Molecular Dynamics (MD) method, Particle-Particle-Particle-Mesh (P^3M) method, and MC method [2]. In the present study, we employ the conventional MC method, yet try to include the Coulomb interaction as accurately as possible [6].

A. Incorporation of the Coulomb Interaction

After very careful optimization of simulation parameters such as mesh size, time step, etc., our 3D self-consistent Monte Carlo simulator is able to reproduce *simultaneously* both the correct mobility under various impurity densities and the collective excitations at the plasma frequency (Fig. 3). Notice that the former reflects the random agitation and the latter represents the collective motion, and both motions conflict each other which makes MC simulations difficult. The parameter optimization is, thus, crucial for stable simulations. In our case, MC simulations under thermal equilibrium have been performed by artificially turning off the energy-dissipating scattering. The total energy of the system is strictly conserved and could be used as a measure to monitor the accuracy and stability of the simulations [6]. This is important because dissipating scattering always stabilizes simulations no matter what the simulation parameters are chosen.

Furthermore, in order to simulate the degenerate electron gas under high electron densities, it is crucial to take into account of Pauli's exclusion principle for *all* short-range scattering in MC simulations. Otherwise, electrons always relax locally to the Maxwell-Boltzmann distribution since they are treated as point particles in MC simulations and the Fermi-Dirac distribution could never be achieved.

B. Device Structure and Potential Fluctuations

The double-gate (DG) MOSFETs with various gate lengths are considered in the present 3D MC simulations described above. We have employed relatively large cross-sectional areas of the device to avoid the effects associated with quantum confinements. The device structure and a typical output (potential profile) from the MC simulations are depicted in Fig. 4. Notice that the magnitude of the potential fluctuations in the source and drain are comparable to the plasmon energy (~200 meV) for the electron density of 10^{20} cm^{-3}. Fourier-transforming the potential fluctuations, we have confirmed a peak around the plasma frequency in the power spectrum even under device operations. Also, the potential in the channel region greatly fluctuates depending on the position of electrons due to small number.

Fig. 5 shows a snapshot of the spatial distribution of electrons in the entire device region as a function of kinetic energy from the self-consistent MC simulations. The red symbols represent electrons with kinetic energy higher than 0.2 eV. The electrons spread over wide ranges of energy which reflect the fact that the potential (the conduction band edge) locally fluctuates. The solid line represents the time-averaged potential profile. Since the mobility in the source and drain is realistic in the present MC simulations, the potential drop (resistance) in the source and drain is rather small. For comparison, a similar snapshot of the MC simulations under the fixed potential is also shown in Fig. 5. It is clear that the energy relaxation in the drain is very slow unless the dynamical potential fluctuations due to the long-range part of the Coulomb interaction are taken into account.

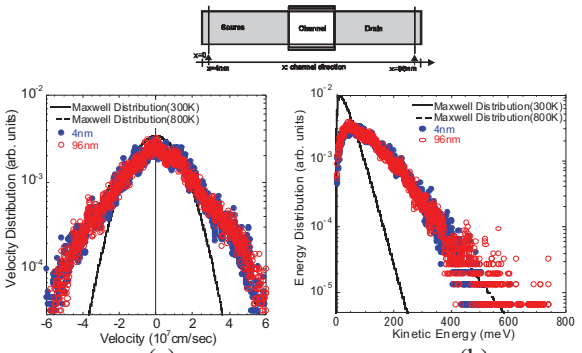

Fig.6. (a) Energy distribution and (b) Velocity distribution close to the ends of the source and drain (see the inset).

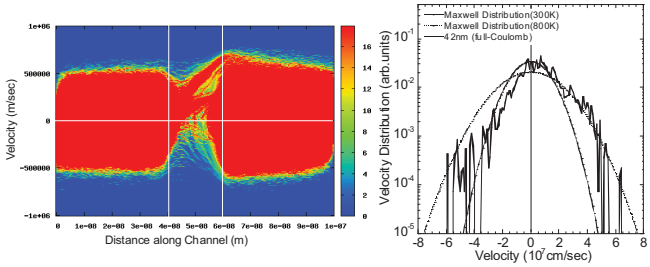

Fig.7. (a) Velocity distribution along the channel direction and (b) Velocity distribution at the virtual source.

C. *Boundary Condition of Distribution Function*

The boundary condition in any transport problems is crucial because the distribution function is continuous. The BTE intrinsically contains dissipation (otherwise, it would not satisfy the H-theorem by Boltzmann) and the distribution function is ought to relax to the (local) thermal equilibrium distribution, that is the only known boundary condition we could impose on solving the BTE.

The consistency of the boundary condition of the distribution function near the contacts in source and drain is confirmed in Fig. 6 for L_c = 20 nm, where the velocity and energy distributions near the source and drain ends are plotted. The shape of the energy distribution in Fig. 6 differs from the thermal equilibrium. This is because it includes both the density of states and potential fluctuations. If the potential fluctuations are de-convoluted from the energy distribution, the energy distribution in Fig. 6 coincides with the Fermi-Dirac distribution.

D. *Quasi-ballistic Transport and Coulomb Interaction*

The velocity distribution along the channel direction is shown in Fig. 7. Two quasi-ballistic flows in the channel are observed. The most important features are; (1) electrons injected into the drain immediately relax into quasi-thermal equilibrium in c.a. 10 nm, and (2) electrons in the source and drain are highly degenerate. The velocity distribution at the virtual source is also shown in Fig. 7. The velocity distribution in the positive regime greatly spreads due to degeneracy in the source, whereas that in the negative regime is close to thermal equilibrium with T = 300 K except the neighborhood of zero velocity where nonequilibrium is very strong. This is consistent with the prediction by the BL theory.

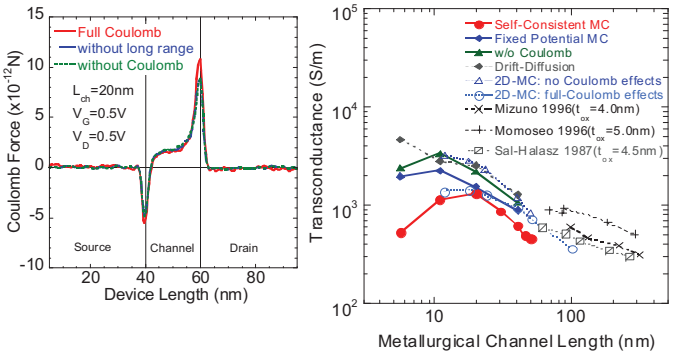

Fig.8. (a) Averaged Coulomb force experienced by an electron and (b) Transconductance as a function of channel length under various MCs.

The strength of the Coulomb force experienced by an electron inside the device and transconductance as a function of gate length are shown in Fig. 8. It is clear that the device performance degradation is observed around L_c = 20 nm, which is consistent with the findings from the previous 2D MC simulations [2]. The degradation is most significant when MC simulations are carried out self-consistently. Therefore, the (long-range) Coulomb interaction would greatly degrade device performance.

IV. Conclusion

The boundary layer due to the singularity of the BTE has been reviewed and its physical interpretation for quasi-ballistic transport has been clarified. The self-consistent 3D MC device simulator including the full Coulomb interaction has been constructed. We have demonstrated that the boundary condition of the electron distribution function plays an essential role to obtain the correct transport characteristics and that the Coulomb interaction is indeed a key ingredient for reliable predictions of device properties.

Acknowledgment

The author is grateful to M. V. Fischetti, S. E. Laux, and T-w. Tang for their fruitful discussion and encouragement.

References

[1] A. Khakifirooz and D. A. Antoniadis, "MOSFET Performance scaling – Part I: Historical trends," IEEE Trans. Electron Devices, ED-55, pp. 1391-1400, June 2008.

[2] M. V. Fischetti et al., "Scaling MOSFETs to 10 nm: Coulomb effects, source starvation, and virtual source model," J. Comp. Electron., pp.60-77 (2009).

[3] N. Sano, "Kinetic of quasiballistic transport in nanoscale semiconductor structures: Is the ballistic limit attainable at room temperature?," Phys. Rev. Lett., 93, pp. 246803-1-4 (2004).

[4] E. Gnani, A. Gnudi, S. Reggiani,G. Baccarani, "Quasi-ballistic transport in nanowire field-effect transistors," IEEE Trans. Electron. Devices 55, pp. 2918–2930 (2008).

[5] M. Lundstrom, "Elementary Scattering Theory of the SiMOSFET," IEEE Electron. Devices Lett., 18, pp. 361–363 (1997).

[6] K, Nakanishi, T. Uechi, N. Sano, "Self-consistent Monte Carlo device simulations under nano-scale device structures: Role of Coulomb interaction, degeneracy, and boundary condition," IEDM Tech. Dig., pp. 79-82 (2009).